Behavior of heavy particles in isotropic turbulence

Jaedal Jung, Kyongmin Yeo,* and Changhoon Lee†
Department of Mechanical Engineering, Yonsei University, 134 Shinchon-dong, Seodaemun-gu Seoul, 120-749, Korea
(Received 30 August 2007; revised manuscript received 17 December 2007; published 23 January 2008)

The motion of heavy particles in isotropic turbulence is investigated using direct numerical simulation. The statistics related to the velocity and acceleration of heavy particles for a wide range of Stokes numbers, defined as the ratio of the particle response time to the Kolmogorov time scale of turbulence ($\mathrm{St}=\tau_p/\tau_\eta$), are investigated. A particular emphasis is placed on the statistics of the fluid experienced by heavy particles, which provide essential information on the dispersion of these particles. The integral time scale of the velocity correlation of fluid seen by the particles T_f, which determines the diffusivity of heavy particles, displays a complex behavior different from the Lagrangian integral time scale of fluid T_L. A plausible physical explanation for the behavior of the time scale is provided.

DOI: 10.1103/PhysRevE.77.016307 PACS number(s): 47.55.Kf, 47.27.E−

I. INTRODUCTION

Heavy particles suspended in turbulence are frequently observed in nature. The behavior of these particles is quite different from that of fluid particles due to differences in the inertia, thus attracting much interest. The most striking phenomenon is the preferential distribution of inertial particles. Heavy particles have been known to accumulate in regions of low vorticity and high strain rate [1–4]. Recent numerical simulations of particle-laden turbulence [5] and helical model flow [6] show that heavy particles are trapped by or expelled from vortical structures, depending on the relative ratio of time scales. This phenomenon has been observed in recent experiments as well [7,8]. Even the anomaly in the Lagrangian structure function was attributed to the trapping of heavy particles in vortex filaments [9].

In an early attempt to describe the dispersion of heavy particles by Tchen (see [10]), the eccentric excursion of heavy particles by vortical structures was not considered, so T_f was assumed to be the same as T_L, thus leading to the result that diffusivity of heavy particles is equal to that of fluid particles, which is obviously not correct. Yudine [11] and Csanady [12] theoretically demonstrated the "crossing trajectories effect" for particles settling under gravity and proposed expressions for T_f. Squires and Eaton [13] performed direct numerical simulation (DNS) of particle-laden isotropic turbulence, but did not recognize the role of T_f in the dispersion of heavy particles. Wang and Stock [14] and Pozorski and Minier [15] noticed the importance of the deviation of T_f from T_L and suggested approximate forms for T_f. However, the flows considered by Wang and Stock and Pozorski and Minier were model flows generated using a stochastic model. Recent DNS of particle-laden isotropic turbulence by He *et al.* [16] provided T_f as a function of the Stokes number without noticing the relevance of the diffusivity of heavy particles. Similarly, Marchioli *et al.* [17] investigated in their DNS of particle-laden channel flow the behavior of T_f, but could not explain the excursion of the particle-to-fluid Reynolds stress from Tchen's prediction because of the extra difficulty of wall-normal inhomogeneity. Considering the volume of particle-laden turbulence research, it is amazing to realize that the correct characterization of the diffusivity of heavy particles in terms of integral time scales, even for simple flows such as isotropic turbulence, has never been provided. Furthermore, a detailed physical explanation of the different behaviors of heavy particles for different Stokes numbers and their implications in dispersion modeling is lacking. Considering that for the prediction of a particle's dispersion, information on the behavior of fluid at the location of the particle is essential, a detailed investigation of the statistical properties of the fluid information along the particle's trajectory is necessary.

In this paper, we investigate the characteristics of heavy particle dispersion, and the statistics of the fluid experienced by the particle in isotropic turbulence for a range of Stokes numbers ($\mathrm{St}=0.1-80$). In our study, we do not take into account the modification of turbulence by heavy particles and the effects of gravity. We extend Tchen's theory by providing a more reasonable approximation for the velocity correlation function considered the relative importance of the Kolmogorov time scale to the particle response time and compare the theoretical predictions of various statistics with our DNS data. A plausible physical explanation of the complicated behavior of the integral time scale of the velocity of fluid seen by particles is provided in detail. Furthermore, considering that acceleration plays an important role in the motion of particles relative to a fluid [18–21], statistics of the accelerations which cause eccentric particle motions are also provided.

II. NUMERICAL SIMULATIONS

For an incompressible turbulent flow, the continuity equation and the Navier-Stokes equations read

$$\frac{\partial u_i}{\partial x_i}=0, \tag{1}$$

*Present address: Division of Applied Mathematics, Brown University, 182 George St., Providence, RI 02912, USA.
†Corresponding author. clee@yonsei.ac.kr

TABLE I. Forcing parameters.

K_F	T_F	ϵ_F
$2\sqrt{2}$	0.4312	0.055

$$\frac{\partial u_i}{\partial t} + \frac{\partial (u_i u_j)}{\partial x_j} = -\frac{\partial p}{\partial x_i} + \nu \frac{\partial^2 u_i}{\partial x_j \partial x_j} + F_i, \tag{2}$$

where x_i and u_i denote the coordinates and the velocity components, p is the pressure, ν is the kinematic viscosity, and F_i is an external forcing. The periodic boundary condition is imposed in all directions. Direct numerical simulations of isotropic turbulence at $\mathrm{Re}_\lambda = 47$ with various Stokes numbers $(0.1-80)$, where Re_λ denotes the Taylor-scale Reynolds number, were performed to investigate the behavior of heavy particles. Although the Reynolds number of the current simulation was low compared to other studies [9,18], it was enough to observe a variety of behaviors of heavy particle motion relative to St and understand the physics of particle-laden turbulence. Furthermore, the Lagrangian statistics, such as acceleration statistics, show a weak dependency on the Reynolds number except for high-order quantities [18]. The computational domain was a cube of side L $(=2\pi)$ with 64^3 grid points, and the governing equations were spatially discretized using the spectral numerical scheme in three dimensions. The viscous terms were treated analytically with an exponential function, and an explicit third-order Runge-Kutta scheme was employed for the nonlinear terms. For the maintenance of stationarity, the forcing scheme provided by Eswaran and Pope [22] was adopted. The Fourier mode of the forcing $\hat{F}_i$ is nonzero for low wave numbers $\underline{k}$ satisfying $0 < \underline{k} \leq K_F$, in which K_F is the maximum wave number of the forced modes, and is determined from the projection of $\hat{b}$ onto the plane normal to wave numbers k in order to guarantee the divergence-free condition

$$\hat{F}_i = \hat{b}_j \delta_{ij} - k_i k_j \hat{b}_j / k^2, \tag{3}$$

where δ_{ij} is the Kronecker delta. $\hat{b}$ is composed of six independent Uhlenbeck-Ornstein random processes with time scale T_F and variance σ_F^2, determined by

$$d\hat{b}_j = -\frac{\hat{b}_j}{T_F} dt + \left(\frac{\sigma_F^2}{T_F}\right) dW, \tag{4}$$

where $\sigma_F^2 = \epsilon_F / T_F$ and dW denotes a randomly chosen number from the normal distribution $(\langle dW \rangle = 0,\ \langle dW^2 \rangle = 1)$.

Under the assumption that particle density is much larger than the fluid density $(\rho_p / \rho_f \geq 100)$, all the transient drags including the added mass and history terms are negligible in the BBO (Basset-Boussinesq-Oseen) equation of motion [23], so the equation for particle motion is simplified to

$$\frac{du_p}{dt} = \frac{1}{\tau_p}(u_f - u_p), \tag{5}$$

$$\tau_p = \rho_p d_p^2 / 18\mu, \tag{6}$$

where u_p is the instantaneous particle velocity, and u_f is the instantaneous fluid velocity at the particle location. The subscript for the vector quantity is dropped for simplicity. τ_p denotes the response time scale of a particle, and d_p and μ are the diameter of the particle and the surrounding fluid's dynamic viscosity, respectively. Note that this equation is valid only when the particle Reynolds number $(\mathrm{Re}_p = d_p \rho_f |u_f - u_p| / \mu)$ is smaller than 1. On the other hand, the particle Reynolds number can be estimated as

$$\mathrm{Re}_p = O\left(\frac{d_p}{\eta} \mathrm{Re}_\lambda \frac{\eta}{\lambda}\right), \tag{7}$$

which is smaller than 1 if $d_p / \eta < (\mathrm{Re}_\lambda\ \eta / \lambda)^{-1} \ll 1$. Hence, the linear drag law can be applied to each of the particles in the momentum equations [2,4]. To obtain statistically convergent data, 2×10^6 particles were released and tracked. To obtain flow quantities such as velocity and acceleration at the locations of the particles, the four-point Hermite interpolation scheme was used in three dimensions, while particles were tracked using the third-order Runge-Kutta time advancement scheme [24].

The forcing parameters K_F, T_F, and ϵ_F, are listed in Table I. These parameters determine not only the flow properties, but also the small-scale resolution in forced isotropic turbulence. Fundamental quantities of the flow field are displayed in Table II. The three length scales are the integral scale

$$l = \frac{\pi}{2u'^2} \int_0^{k_{\max}} k^{-1} E(k) dk, \tag{8}$$

the Kolmogorov microscale

$$\eta = (\nu^3 / \epsilon)^{1/4}, \tag{9}$$

and the Taylor microscale:

$$\lambda = (15\nu / \epsilon)^{1/2} u', \tag{10}$$

where $E(k)$ is the energy spectrum, u' is the root-mean-squared velocity, and ϵ is the energy dissipation rate.

The minimum requirement for the spatial resolution is that $k_{\max} \eta \geq 1.0$, where $k_{\max}$ $(=\sqrt{2} N k_1 / 3,)$ is the largest wave number, and the lowest wave number k_1 is equal to $2\pi / L$ [22]. In our study, $k_{\max} \eta = 1.24$.

III. LAGRANGIAN AUTOCORRELATION FUNCTION

In this section we investigate in detail the autocorrelation functions of velocity and acceleration, and the relevant time

TABLE II. Flow properties from the simulations.

N	Re_λ	ν	ϵ	u'	l	η	λ	$k_{\max}\eta$	l/η	τ_η
64^3	46.9	0.03	9.43	2.54	1.08	0.04	0.55	1.24	26.32	0.0564

scales. The autocorrelation functions of velocity and acceleration are defined as

$$\rho(t) = \frac{\langle u(t_0)u(t+t_0)\rangle}{\langle u^2(t_0)\rangle}, \tag{11}$$

$$\rho^a(t) = \frac{\langle a(t_0)a(t+t_0)\rangle}{\langle a^2(t_0)\rangle}, \tag{12}$$

where the subscript for the vector quantity is dropped for simplicity, and t_0 is the reference time. The bracket $\langle\ \rangle$ denotes the ensemble-averaged quantity. Similarly, the autocorrelation functions of inertial particles $\rho_p(t)$ and $\rho_p^a(t)$, and those of fluid particles seen by the inertial particles $\rho_f(t)$ and $\rho_f^a(t)$, are defined by u_p and a_p, and u_f and a_f, respectively. The corresponding integral time scales of the velocity autocorrelation are defined as

$$T_L = \int_0^\infty \rho(t)dt, \tag{13}$$

$$T_p = \int_0^\infty \rho_p(t)dt, \tag{14}$$

$$T_f = \int_0^\infty \rho_f(t)dt. \tag{15}$$

The original Tchen's theory (see [10]) is based on the assumption that during the motion of the particle, its neighborhood will be formed by the same fluid, leading to the result that no distinction between the Lagrangian fluid particle and the fluid particle as seen by the inertial particle is made, and thus

$$\rho_f = \rho = \exp(-t/T_L), \tag{16}$$

which implies that $T_f = T_L$, which is not exactly true as will be shown below. A simple correction is possible using T_f. The modified expression is

$$\rho_f = \exp(-t/T_f). \tag{17}$$

A more refined model is considered by noticing that the behavior of the correlation function at the origin can be better represented by adopting a double exponential distribution using the Kolmogorov time scale,

$$\rho_f = \frac{T'\exp(-t/T') - \tau_\eta \exp(-t/\tau_\eta)}{T' - \tau_\eta} \quad \text{[see Eq. (A1)]}, \tag{18}$$

where $T' = T_f - \tau_\eta$. Given that the Stokes number can be smaller than 1, a correct representation of the correlation function over a short time on the order of the Kolmogorov time scale would result in better prediction of a particle's behavior. A similar approach was taken by Sawford [25] in the development of stochastic models for acceleration. We will refer to each approach as the original Tchen's analysis (OT), the modified Tchen's analysis (MT), and the refined Tchen's analysis (RT), respectively. Figure 1 clearly shows

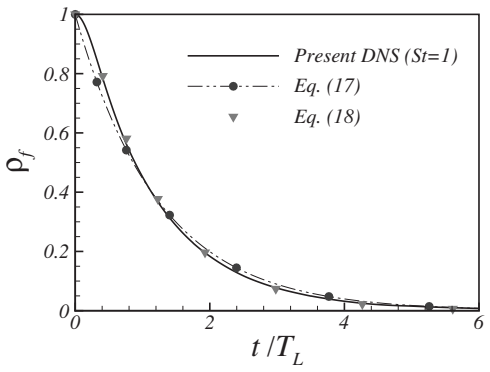

FIG. 1. Comparison of the present ρ_f and the Tchen's ρ_f at St=1.

that the refined Tchen's ρ_f at St=1 better approximates DNS data.

The root-mean-squared velocities of suspended particles and the fluid experienced by the particles are obtained for each analysis as follows:

$$\frac{\langle u_p^2\rangle}{\langle u_f^2\rangle} = \frac{T_L/\tau_p}{1 + T_L/\tau_p} \quad \text{(OT)}, \tag{19}$$

$$\frac{\langle u_p^2\rangle}{\langle u_f^2\rangle} = \frac{T_f/\tau_p}{1 + T_f/\tau_p} \quad \text{(MT)}, \tag{20}$$

$$\frac{\langle u_p^2\rangle}{\langle u_f^2\rangle} = \frac{\tau_\eta(\tau_p + T') + \tau_p T'}{(\tau_\eta + \tau_p)(\tau_p + T')} \quad \text{(RT)} \quad \text{[see Eq. (A7)]}, \tag{21}$$

which are shown in Fig. 2 along with the DNS prediction. The prediction of the refined Tchen's analysis [Eq. (21)] shows better agreement with DNS.

Figure 3 shows the effect of inertia on the autocorrelation of the heavy particle velocity ρ_p. The predictions of the modified and refined Tchen's analyses are obtained from Eqs. (17) and (18) as follows:

$$\rho_p = \frac{(T_f/\tau_p)\exp(-t/T_f) - \exp(-t/\tau_p)}{T_f/\tau_p - 1} \quad \text{(MT)}, \tag{22}$$

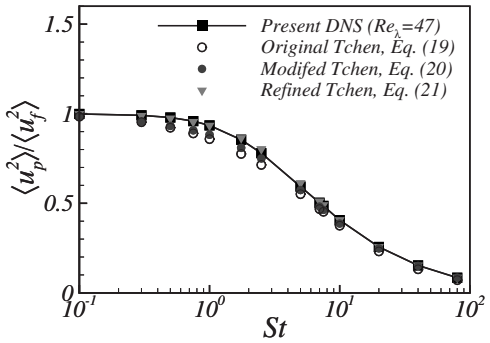

FIG. 2. Effect of various St on $\langle u_p^2\rangle/\langle u_f^2\rangle$.

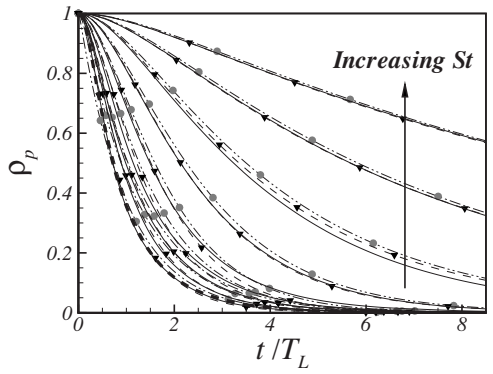

FIG. 3. Effect of inertia on the Lagrangian velocity autocorrelation function of the heavy particle at St=0.1,0.5,1,2.5, 5,10,20,40,80. The fluid particle (dashed line), the modified Tchen's particle correlation [●, Eq. (21)], and the refined Tchen's particle correlation [▲, Eq. (22)].

$$\rho_p = \frac{e^{-t/T'}(\tau_\eta^2 - \tau_p^2)T'^3 + e^{-t/\tau_\eta}(\tau_p^2 - T'^2)\tau_\eta^3 + e^{-t/\tau_p}(T'^2 - \tau_\eta^2)\tau_p^3}{(\tau_\eta - \tau_p)(\tau_\eta - T')(\tau_p - T')[\tau_p T' + \tau_\eta(\tau_p + T')]}$$

(RT) [see Eq. (A8)], (23)

and are shown for comparison. The original Tchen's analysis yields the same relation for ρ_p as Eq. (22) with T_f replaced by T_L, which is not shown in Fig. 3 due to the large deviation from the DNS results. As shown in Fig. 3, ρ_p extends further as the Stokes number increases for the obvious reason that a heavier particle has more inertia [13].

On the other hand, the autocorrelation of the fluid velocity seen by the particles displays quite a different behavior from that of inertial particles as illustrated in Fig. 4. It varies between two limiting correlations, the Lagrangian fluid correlation and the Eulerian correlation [14]. Three different regimes of the Stokes number are noticeable: for $0<\mathrm{St}\leq 1$, ρ_f increases, for $1<\mathrm{St}<10$, ρ_f decreases, and for $10\leq \mathrm{St}<\infty$, ρ_f increases again. A plausible physical explanation for this is provided in Fig. 5, which associates the relative motion of a suspended particle with a rotating vortical flow structure. As $\mathrm{St}\to 0$, a suspended particle shows no distinction from a fluid particle so that the particle near a vortical structure follows a streamline around the vortex [see Fig. 5(a)], and the autocorrelation reduces to the Lagrangian fluid correlation. As the particle inertia increases ($0<\mathrm{St}\leq 1$), the deviation from the fluid path becomes more pronounced. The particle with inertia near a vortex tends to deviate from the vortex streamline due to the centrifugal force induced by the swirling flow [2,3]. Compared to the limiting case where a suspended particle follows the Lagrangian path of a fluid particle, which displays short correlation due to the change in direction of velocity along the circumferential path [Fig. 5(a)], a particle with inertia will experience a less-curved path along which fluid information does not change so quickly [Fig. 5(b)]. Subsequently, the autocorrelation of the velocity of fluid seen by the particle, increases as shown in Fig. 4(a). This is consistent with the well-known fact that heavy particles tend to concentrate in a preferential region of high strain and low vorticity [4]. It seems quite reasonable

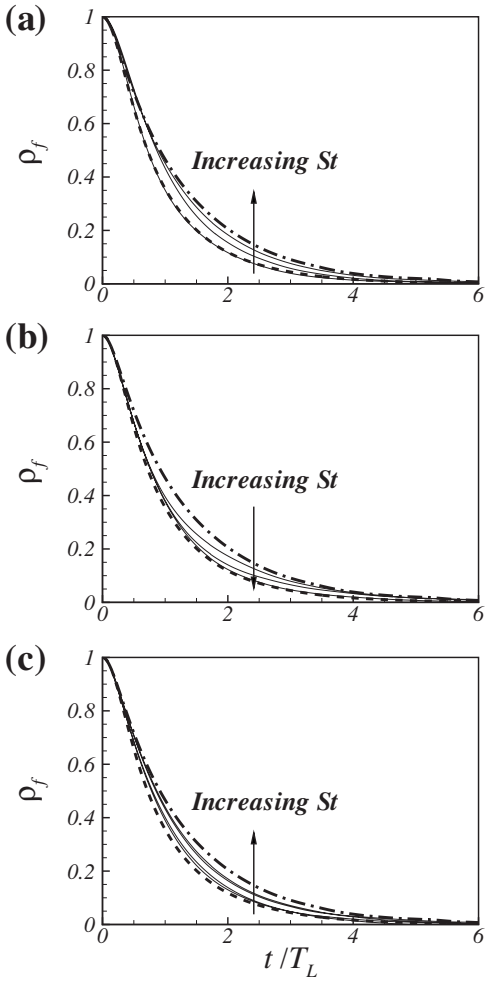

FIG. 4. Effect of inertia on the Lagrangian velocity autocorrelation of the fluid seen by particles. Lagrangian fluid velocity autocorrelation (dashed line) and Eulerian fluid velocity autocorrelation (dash-dotted line). (a) St=0.1,0.5,1; (b) St=2.5,5,7.5; and (c) St =10,20,40,80.

that this deviation of the velocity autocorrelation from the Lagrangian fluid correlation has a maximum at St=1, considering that the interaction between a suspended particle and the background turbulence is maximized when the relevant time scales, the response time scale of the particle, and

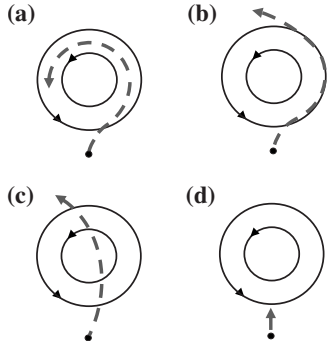

FIG. 5. Four regimes of heavy particle motion. (a) $\mathrm{St}\to 0$; (b) $0<\mathrm{St}\leq 1$; (c) $1<\mathrm{St}\lesssim T_L/\tau_\eta$ ($\langle u_p^2\rangle/\langle u_f^2\rangle \approx 0.5$); and (d) $\mathrm{St}\to\infty$.

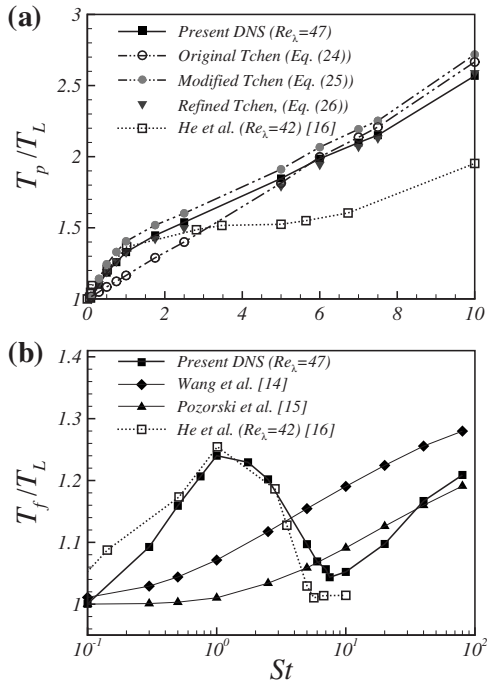

FIG. 6. Effect of inertia on the Lagrangian integral time scale of the heavy particle and the fluid seen by particles, normalized by the Lagrangian integral time scale.

the Kolmogorov time scale are the same. When a particle has too much inertia, however, any interaction between the particle and a flow structure becomes unlikely. A particle can simply cross the vortical structure [Fig. 5(c)], the result being that the velocity of fluid seen by the particle has less correlation than the case in which it has maximum interaction. This phenomenon is observed for $\mathrm{St} \approx T_L/\tau_\eta$, and is in some sense similar to the "crossing trajectory effect" for inertial particles settling under gravity. A further increase of the Stokes number, however, leads to a significant suppression of the velocity of inertial particles (Fig. 2), implying that the particles rarely move [Fig. 5(d)]. Then the autocorrelation of fluid experienced by the particle recovers the Eulerian correlation as shown in Fig. 4(c).

A more quantitative analysis of the autocorrelation can be carried out through an investigation of the integral time scale. Figure 6 shows the integral time scales of the autocorrelations of inertial particles T_p, and of the fluid seen by particles T_f. For T_p, our DNS results along with data available from previous studies are compared to predictions from the original, modified, and refined Tchen's analyses, which are

$$T_p = T_L + \tau_p \quad \text{(OT)}, \tag{24}$$

$$T_p = T_f + \tau_p \quad \text{(MT)}, \tag{25}$$

$$T_p = \frac{(\tau_\eta + \tau_p)(\tau_\eta + T')(\tau_p + T')}{\tau_p T' + \tau_\eta(\tau_p + T')} \quad \text{(RT)} \quad [\text{see Eq. (A9)}]. \tag{26}$$

The prediction of the refined Tchen's analysis best fits the DNS data, and the major difference between the original Tchen's analysis and the other analysis originates from the difference between T_L and T_f. Although the present Re_λ is similar to that of He *et al.* [16], a large discrepancy in T_p between our DNS and He *et al.*'s DNS data obtained using a lower-order interpolation scheme can be seen.

A detailed distribution of T_f obtained from our DNS is shown in Fig. 6(b). Also, the formulas for T_f suggested by Wang and Stock [14], and Pozorski and Minier [15] are compared to the present T_f. Pozorski and Minier modified the existing Langevin model for instantaneous relative velocity (LIV) to satisfy the two limiting cases: $T_f = T_L$ for $\mathrm{St} \to 0$, and $T_f = T_E$ for $\mathrm{St} \to \infty$, so that the Langevin formula consists of respective Langevin equations using T_L and T_E. The relation between T_E, T_L, and T_f in the modified LIV model is as follows:

$$\frac{1}{T_f} = \frac{x}{T_L} + \frac{1-x}{T_E}, \tag{27}$$

where x denotes the ratio of the particle's rms velocity to the fluid's rms velocity seen by the particle. Wang and Stock [14] also performed a numerical simulation using a stochastic model for the Gaussian random velocity field, and then suggested T_f by curve fitting their results using the assumption $T_E u'/l = 1$,

$$T_f = T_E\left(1 - \frac{0.664}{(1+\mathrm{St})^{0.4(1+0.01\mathrm{St})}}\right). \tag{28}$$

Obviously, their formulas [Eqs. (27) and (28)] cannot capture the N-shape distribution of T_f, although the limiting behaviors for $\mathrm{St} \to 0$ and $\mathrm{St} \to \infty$ are correct. Considering that the most interesting physical behavior occurs near $\mathrm{St} = 1$ and the information provided by T_f directly influences the diffusivity of inertial particles, which will be shown below, a correct prediction for T_f is very important.

By curve fitting, we propose a new formula for T_f, which not only satisfies the two limiting values but also captures the oscillatory behavior around $\mathrm{St} = 1$.

$$\frac{T_f}{T_L} = 0.245 e^{-[\ln(\mathrm{St}/1.2)/1.3]^2} + \frac{[1 + (T_E/T_L)(0.025\ \mathrm{St})^{1.5}]}{1 + (0.025\ \mathrm{St})^{1.5}}. \tag{29}$$

This formula is compared to our DNS data in Fig. 7.

Accelerations of inertial particles or fluid particles, which directly determine the relative motion of inertial particles, might reveal some characteristics of particle diffusion. The acceleration autocorrelations of inertial particles and of fluid seen by the particles are shown in Fig. 8 along with the Lagrangian fluid acceleration autocorrelation. The autocorrelation of inertial particles ρ_p^a, monotonically increases as St increases, while the autocorrelation of fluid seen by the particles is relatively insensitive to St. The behavior of ρ_p^a is predictable since, as the particle inertia increases, the particle velocity tends to maintain the original value and then the force acting on the particle does not change quickly, the result being that the acceleration has longer correlation. A more detailed investigation of the autocorrelation of fluid seen by the particles ρ_f^a, was carried out through the investigation of the zero-crossing time of the correlation, the behav-

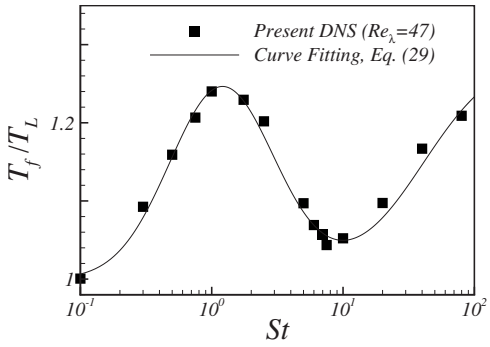

FIG. 7. The curve fitting of the integral time scale of the fluid seen by a heavy particle as a function of St.

ior of which is shown in the inset of Fig. 8(b). Here, the zero-crossing time $t0$ of the Lagrangian fluid acceleration correlation is approximately $0.355T_L$, which agrees with the result $2.2\tau_\eta$ of Yeung and Pope [26]. Compared to this value, the zero-crossing time of the fluid seen by lighter particles (St$\leq$1) is longer, and that of heavier particles (St$>$1) is shorter. This can be understood through the investigation of the relative motion of inertial particles near a vortical structure, as in the explanation of the velocity autocorrelations. The zero-crossing time usually indicates the time span over which a fluid particle completes one-fourth of a full swirling motion, so that the direction of the centripetal acceleration changes by 90°. As the particle inertia increases from St=0, the inertial particle tends to deviate from the swirling motion

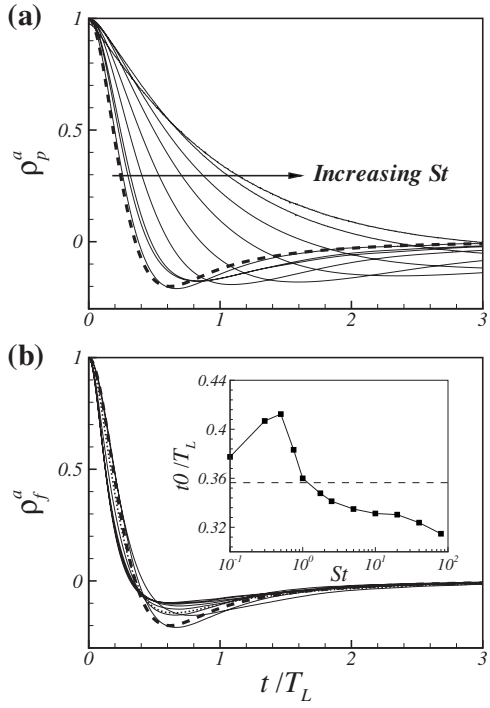

FIG. 8. Effect of inertia on the Lagrangian acceleration autocorrelation of the heavy particle and the fluid seen by the particle along with the Lagrangian fluid acceleration autocorrelation (dashed line). St=0.1,0.5,1 (dotted line), 2.5, 5, 10, 20, 40, 80. The inset indicates the zero-crossing time of the fluid seen by particles.

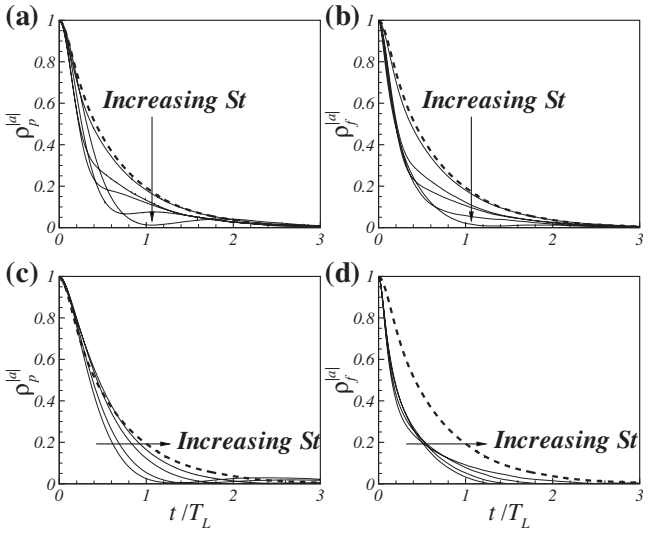

FIG. 9. Effect of inertia on the Lagrangian acceleration magnitude autocorrelation of the heavy particle and the fluid seen by the particle along with the Lagrangian fluid acceleration magnitude autocorrelation (dashed line). (a) and (b) St=0.1,0.5,1,2.5,5. (c) and (d) St=7.5,10,20,40.

of fluid due to inertia, thus creating a less-curved trajectory, so that the time for the change of acceleration direction becomes longer. However, when the particle inertia becomes too large, the particle is no longer influenced by the swirling motion of fluid, so the fluid information seen by the particle becomes uncorrelated. It is interesting to note that those effects are canceled near St=1, so that the zero-crossing time of ρ_f^a is the same as that of the Lagrangian fluid acceleration correlation.

The correlation of the acceleration magnitude is usually much longer than the correlation of the acceleration components because the magnitude of the centripetal acceleration near the vortical structure persists for quite a long time, while the direction of acceleration quickly changes. Figure 9 shows the autocorrelations of the acceleration magnitude of a heavy particle $\rho_p^{|a|}$, and of the fluid seen by the particle, $\rho_f^{|a|}$. As St increases from 0 to 5, both correlations decrease from the Lagrangian fluid autocorrelation of the acceleration magnitude and $\rho_p^{|a|}$ increases with a further increase of St, whereas $\rho_f^{|a|}$ retains almost the same distribution as that at St=5. The initial decreases are probably due to the deviation of inertial particles from the swirling motion associated with the vortical structure as the particle inertia increases. As St increases further, the particle path becomes irrelevant to the flow structure, thus $\rho_f^{|a|}$ should remain uncorrelated, while $\rho_p^{|a|}$ increases due to the increase of the particle inertia.

IV. DISPERSION OF HEAVY PARTICLES

The dispersion of inertial particles is defined as the ensemble-averaged displacements of the particles relative to their initial positions,

$$\sigma_X^2(t) = \langle [X(t_0+t) - X(t_0)]^2 \rangle. \tag{30}$$

According to Taylor's theory for stationary isotropic turbulence, the dispersion can be approximated by

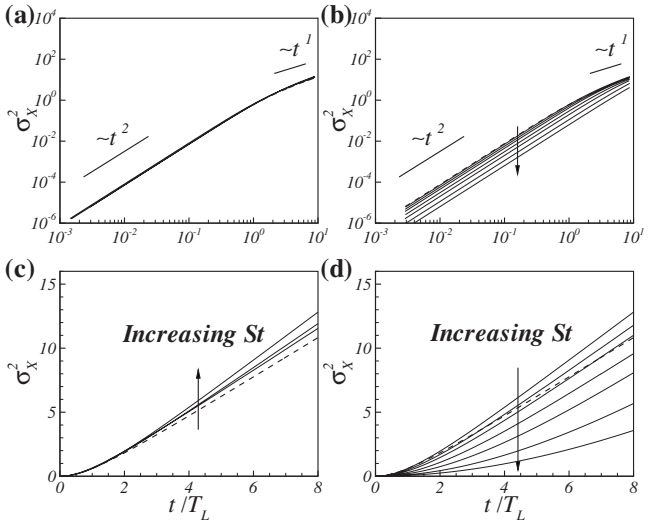

FIG. 10. The mean-square dispersions of heavy particles and of fluid particles (dashed line). (a) and (b) The log-log scale. (c) and (d) The normal scale. St=0.1,0.5,1 (left), and St=1,2.5,5, 10,20,40,80 (right).

$$\sigma_X^2(t) \approx \langle u_p^2 \rangle t^2 \quad \text{for } t \ll T_p, \tag{31}$$

$$\sigma_X^2(t) \approx 2\langle u_p^2 \rangle T_p t \quad \text{for } t \gg T_p. \tag{32}$$

Figure 10 illustrates the mean square dispersion of heavy particles on the log-log scale (a,b), and on the normal scale (c,d) for various Stokes numbers. For lighter particles (St ≤ 1), the early behavior of the dispersion is not much different from the dispersion of the Lagrangian fluid particles, whereas for heavier particles (St >1), the dispersion itself is suppressed and the initial period during which the dispersion quadratically increases extends further. This is because $\langle u_p^2 \rangle$ decreases and T_p increases as the Stokes number increases [Figs. 2 and 6].

By Batchelor's theory [27], the eddy diffusivity of inertial particles defined by the dispersion can be related to the integral time scale as follows:

$$D_p \equiv \frac{1}{2}\frac{d\sigma_X^2}{dt} = \langle u_p^2 \rangle T_p \tag{33}$$

for $t \gg T_p$. Figure 11 shows D_p/D, where D is the eddy diffusivity of fluid particles, along with the predictions of the modified and refined Tchen's analyses and other previous data. By definition,

$$\frac{D_p}{D} = \frac{\langle u_p^2 \rangle T_p}{\langle u_f^2 \rangle T_L} = \frac{T_f}{T_L} \quad \text{(MT,RT)} \quad \text{[see Eq. (A10)]}, \tag{34}$$

where the second relation follows from Eqs. (20) and (25) for the modified Tchen's analysis and Eqs. (21) and (26) for the refined Tchen's analysis. This simply states that the deviation of diffusivity of the inertial particles from that of fluid particles comes from the difference between the integral time scale of the correlation of fluid seen by the inertial particles and the Lagrangian integral time scale of fluid particles. The peak diffusivity around St=1 seems to be because $\langle u_p^2 \rangle$ hardly changes up to St=1 (Fig. 2) while T_p monotonically increases with St [Fig. 6(a)]. Considering that this insensitive behavior of $\langle u_p^2 \rangle$ results from the outward ejection of inertial particles by the swirling motion of vortex structures, it can be conjectured that coherent structures enhance the dispersion of particles [28]. On further increase of St, D_p/D increases again and approaches T_E/T_L [14].

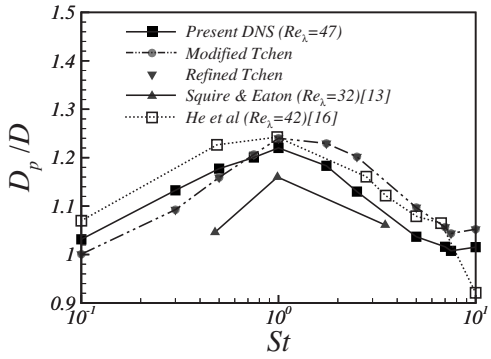

FIG. 11. Eddy diffusivity of heavy particles.

V. CONCLUSIONS

The behavior of suspended heavy particles and of the fluid experienced by the particles in forced isotropic turbulence at $\mathrm{Re}_\lambda=47$ was investigated using direct numerical simulation. The excursions of the autocorrelations of velocity, and of the accelerations of inertial particles and fluid seen by the particles from the Lagrangian fluid correlation were explained by the inertial particle's behavior near the coherent vortical structures of background turbulence across a range of the Stokes numbers (St=0.1−80). We also extended Tchen's analysis for particle motion by introducing a more realistic approximation for the velocity correlation function and compared it with our DNS results for various statistics. We found that the deviation of the integral time scale of fluid seen by the inertial particles from the Lagrangian fluid integral time scale is not monotonically varying with the Stokes number, the reason for which was deduced by investigating the relative motion of particles near a rotational vortical structure. This departure was found to uniquely determine the relative diffusivity of inertial particles to that of fluid particles, which shows a peak at St=1.

APPENDIX: REFINED TCHEN'S ANALYSIS

The original Tchen's theory assumed an exponential function $[\rho_f=\exp(-t/T_L)]$ for the autocorrelation of the velocity of fluid seen by inertial particles. As shown in Fig. 1, this form does not capture the behavior near the origin. Thus, we introduce a refined expression for the correlation using a double exponential function, which includes the Kolmogorov time scale of turbulence, as follows:

$$\rho_f = \frac{T' \exp(-t/T') - \tau_\eta \exp(-t/\tau_\eta)}{T' - \tau_\eta}. \tag{A1}$$

The corresponding energy spectrum then becomes

$$E_f(n) \equiv \frac{2}{\pi}\int_0^\infty \rho_f \cos(2\pi n t)dt = 4\langle u_f^2\rangle \frac{T' + \tau_\eta}{(1 + T'^2\omega^2)(1 + \tau_\eta^2\omega^2)}, \tag{A2}$$

where $n = \omega/2\pi$ and ω is the frequency.

In order to relate the energy spectrum of an inertial particle $E_p(n)$ to $E_f(n)$, we express u_p and u_f as a Fourier integral,

$$u_f = \int_0^\infty (\alpha \cos \omega t + \beta \sin \omega t)d\omega,$$

$$u_p = \int_0^\infty (\gamma \cos \omega t + \delta \sin \omega t)d\omega. \tag{A3}$$

Using Eq. (6) and comparing coefficients, we obtain the following relations between γ and δ, and α and β:

$$\gamma = [1 + f_1(\omega)]\alpha + f_2(\omega)\beta,$$

$$\delta = [1 + f_1(\omega)]\beta - f_2(\omega)\alpha, \tag{A4}$$

where

$$f_1(\omega) = -\frac{\omega^2}{1/\tau_p^2 + \omega^2}, \quad f_2(\omega) = -\frac{\omega/\tau_p}{1/\tau_p^2 + \omega^2}. \tag{A5}$$

Rearranging yields

$$E_p(n)/E_f(n) = (\gamma^2 + \delta^2)/(\alpha^2 + \beta^2) = [1 + f_1(\omega)]^2 + f_2^2(\omega) = (1/\tau_p^2)/(1/\tau_p^2 + \omega^2), \tag{A6}$$

which leads to

$$\langle u_p^2\rangle = \int_0^\infty E_p(n)dn = \frac{2}{\pi}\langle u_f^2\rangle \int_0^\infty \left[\frac{(T' + \tau_\eta)/\tau_p^2}{(1 + T'^2\omega^2)(1 + \tau_\eta^2\omega^2)(1/\tau_p^2 + \omega^2)}\right]d\omega = \langle u_f^2\rangle \frac{\tau_\eta(\tau_p + T') + \tau_p T'}{(\tau_\eta + \tau_p)(\tau_p + T')}. \tag{A7}$$

On the other hand, the inertial particle correlation ρ_p can be obtained,

$$\rho_p = \frac{1}{\langle u_p^2\rangle}\int_0^\infty (E_p(n)\cos \omega t)dn = \frac{2}{\pi}\frac{\langle u_p^2\rangle}{\langle u_f^2\rangle}\int_0^\infty \left[\frac{(T'^2 + \tau_\eta^2)/\tau_p^2 \cos \omega t}{(1 + T'^2\omega^2)(1 + \tau_\eta^2\omega^2)(1/\tau_p^2 + \omega^2)}\right]d\omega = \frac{e^{-t/T'}(\tau_\eta^2 - \tau_p^2)T'^3 + e^{-t/\tau_\eta}(\tau_p^2 - T'^2)\tau_\eta^3 + e^{-t/\tau_p}(T'^2 - \tau_\eta^2)\tau_p^3}{(\tau_\eta - \tau_p)(\tau_\eta - T')(\tau_p - T')[\tau_p T' + \tau_\eta(\tau_p + T')]}, \tag{A8}$$

from which the integral time scale T_p is obtained using

$$T_p = \int_0^\infty \rho_p(t)dt = \frac{(\tau_\eta + \tau_p)(\tau_\eta + T')(\tau_p + T')}{\tau_p T' + \tau_\eta(\tau_p + T')}. \tag{A9}$$

The diffusivity of an inertial particle, Eq. (33), can then be easily obtained from Eqs. (A7) and (A9),

$$D_p/D = \frac{\langle u_p^2\rangle}{\langle u_f^2\rangle}\left(\frac{T_p}{T_L}\right) = \frac{\tau_\eta + T'}{T_L} = \frac{T_f}{T_L}. \tag{A10}$$

[1] M. R. Maxey, Phys. Fluids **30**, 1915 (1987).
[2] K. D. Squires and J. K. Eaton, Phys. Fluids A **2**, 1191 (1990).
[3] K. D. Squires and J. K. Eaton, Phys. Fluids A **3**, 1169 (1991).
[4] L. P. Wang and M. R. Maxey, J. Fluid Mech. **256**, 27 (1993).
[5] L. Biferale, G. Boffetta, A. Celani, A. Lanotte, and F. Toschi, Phys. Fluids **17**, 021701 (2005).
[6] R. H. A. Ijzermans, R. Hagmeijer, and P. V. Langen, Phys. Fluids **19**, 107102 (2007).
[7] T. S. Yang and S. S. Shy, Phys. Fluids **15**, 868 (2003).
[8] A. M. Wood, W. Hwang, and J. K. Eaton, Int. J. Multiphase Flow **31**, 1220 (2005).
[9] J. Bec, L. Biferale, M. Cencini, A. Lanotte, and F. Toschi, Phys. Fluids **18**, 081702 (2006).
[10] J. O. Hinze, *Turbulence*, 2nd ed. (McGraw-Hill, New York, 1975).
[11] M. I. Yudine, Adv. Geophys. **6**, 185 (1959).
[12] G. T. Csanady, J. Atmos. Sci. **20**, 201 (1963).
[13] K. D. Squires and J. K. Eaton, J. Fluid Mech. **226**, 1 (1991).
[14] L. P. Wang and D. E. Stock, J. Atmos. Sci. **50**, 1897 (1993).
[15] J. Pozorski and J. P. Minier, Int. J. Multiphase Flow **24**, 913 (1998).
[16] Z. He, Z. Liu, S. Chen, L. Weng, and C. Zheng, Acta Mech. Sin. **21**, 112 (2005).
[17] C. Marchiloi, M. Picciotto, and A. Soldati, J. Turbul. **7**, 60, (2006).
[18] J. Bec, L. Biferale, G. Boffetta, A. Celani, M. Cencini, A. Lanotte, S. Musacchio, and F. Toschi, J. Fluid Mech. **550**, 349 (2006).
[19] A. La Porta, G. A. Voth, A. M. Crawford, J. Alexander, and E. Bodenschatz, Nature (London) **409**, 1017 (2001).
[20] C. Lee, K. Yeo, and J. I. Choi, Phys. Rev. Lett. **92**, 144502 (2004).
[21] S. Lee and C. Lee, Phys. Rev. E **71**, 056310 (2005).
[22] V. Eswaran and S. B. Pope, Comput. Fluids **16**, 257 (1988).
[23] M. R. Maxey and J. J. Riley, Phys. Fluids **26**, 883 (1983).
[24] J. Choi, K. Yeo, and C. Lee, Phys. Fluids **16**, 779 (2004).
[25] B. L. Sawford, Phys. Fluids A **3**, 1577 (1991).
[26] P. K. Yeung and S. B. Pope, J. Fluid Mech. **207**, 531 (1989).
[27] G. K. Batchelor, Aust. J. Sci. Res., Ser. A **2**, 437 (1949).
[28] J. S. Marshall, Phys. Fluids **17**, 025104 (2005).